Influence of wall thickness on the stability of the resistive wall mode in tokamak plasmas

Richard Fitzpatrick
Department of Physics, Institute for Fusion Studies, University of Texas at Austin, Austin, Texas 78712, USA

(Received 24 October 2012; accepted 14 December 2012; published online 7 January 2013)

The influence of finite wall thickness on the stability of the resistive wall mode (RWM) in a tokamak is determined using a simple cylindrical plasma model in which the dissipation required to stabilize the mode is provided by neoclassical parallel ion viscosity. For present-day tokamaks, which possess relatively thin walls, finite wall thickness effects are found to have relatively little influence on the RWM stability boundaries, which are almost the same as those calculated in the thin-wall limit. On the other hand, for next-step devices, which are likely to possess much thicker walls than present-day tokamaks, finite wall thickness effects are found to significantly impede the ability of plasma rotation to stabilize the RWM all the way to the perfect-wall stability limit. [http://dx.doi.org/10.1063/1.4773907]

I. INTRODUCTION

The promising "advanced tokamak" (AT) concept is only economically attractive provided that the ideal external-kink β-limit is raised substantially due to the presence of a rigid, close-fitting, electrically conducting, wall.[1–3] This, in turn, is only possible provided that the so-called *resistive wall mode* (RWM) is somehow stabilized.[4] Various tokamak experiments have established that the RWM can, in fact, be stabilized by modest levels (i.e., 1% of the Alfvén velocity) of *plasma toroidal rotation*.[5–9] According to conventional theory, this stabilization is a combined effect of plasma *rotational inertia* and plasma *dissipation*.[10,11]

For the sake of simplicity, the majority of previously published theoretical studies of RWM stability in tokamaks have assumed that the wall is "electromagnetically thin" (i.e., that the radial thickness of the wall is much less than the electromagnetic skin-depth in the wall material). This assumption is reasonable for present-day devices, which tend to have relatively thin walls, but is not appropriate to next-step devices, such as ITER,[12] which will necessarily have thick walls (for engineering reasons). The few published RWM studies that have not made the assumption that the wall is electromagnetically thin have concentrated on the effect of wall thickness on the *typical growth-rate* of the instability.[13–15] However, as soon as we accept that any conceivable RWM growth-rate would allow such a mode to grow to a dangerous amplitude in a time that is much less than the lifetime of the plasma discharge, it becomes clear that the central question is the effect of wall thickness on the RWM *stability boundaries*. In other words, the central question is the extent to which a thick wall facilitates, or impedes, the ability of modest levels of plasma toroidal rotation to stabilize the RWM, and, thereby, raise the effective β-limit. The aim of this paper is to address this question directly using a relatively simple cylindrical plasma model in which the dissipation required to stabilize the mode is provided by *neoclassical parallel ion viscosity*.[16–18]

II. DERIVATION OF RWM DISPERSION RELATION

A. Plasma model

Consider a large aspect-ratio, low-β, circular cross-section, tokamak plasma of major radius R_0, minor radius a, on-axis toroidal magnetic field-strength B_0, and on-axis plasma mass density ρ_0. The inverse aspect-ratio of the plasma is $\epsilon_0 = a/R_0$.

In the following, all lengths are normalized to a, all magnetic field-strengths to B_0, and all times to the hydromagnetic time-scale $\tau_H = (R_0/B_0)\sqrt{\mu_0\,\rho_0}$.

The plasma equilibrium is described by the model safety-factor profile

$$q(r) \equiv \frac{r\,\epsilon_0}{B_\theta(r)} = \frac{q_a\,r^2}{1-(1-r^2)^{\,q_a/q_0}}, \tag{1}$$

and the model density profile

$$\rho(r) = (1-r^2)^{\,\alpha}. \tag{2}$$

Here, r is the radial distance from the magnetic axis, q_a the safety factor at the edge of the plasma, and q_0 the safety factor on the magnetic axis.

The plasma response to the near-resonant helical magnetic perturbation generated by a RWM (with, say, m periods in the poloidal direction, and n periods in the toroidal direction) is governed by the eigenmode equation[16–18]

$$\begin{aligned} &r\,\frac{d}{dr}\left[\left(\rho\,\gamma'^2\left[1+\frac{q^2}{\epsilon_0^2}\,\frac{\mu_\parallel}{\gamma'+\mu_\parallel\,r^2}\right]+Q^2\right)r\,\frac{d\phi}{dr}\right]\\ &-\left[m^2\left(\rho\,\gamma'\left[\gamma'+\frac{q^2}{\epsilon_0^2}\,\mu_\parallel\right]+Q^2\right)+r\,\frac{dQ^2}{dr}\right]\phi\\ &=0, \end{aligned} \tag{3}$$

where $\gamma' = \gamma - \mathrm{i}\,n\,\Omega_\phi$ is the mode growth-rate in the plasma frame, γ the growth-rate in the laboratory frame, and Ω_ϕ the

plasma toroidal angular rotation velocity. (Any plasma poloidal rotation is neglected in this paper, for the sake of simplicity. Likewise, Ω_ϕ is assumed to be uniform.) Furthermore, $Q(r) = m/q(r) - n$, and $-\gamma' \phi$ is the perturbed scalar electric potential associated with the RWM. It is assumed that $m \gg n\,\epsilon_0$ (which is a standard large aspect-ratio tokamak ordering). Finally, $\mu_\parallel$ is the *neoclassical parallel ion viscosity*.[16–18] Note that the dissipation due to neoclassical parallel ion viscosity is strongly peaked at the edge of the plasma (where Q is small). Hence, it is a reasonable approximation to set the neoclassical viscosity profile in Eq. (3) to a uniform value characteristic of the viscosity at the edge of the plasma.[17]

Launching a well-behaved solution to Eq. (3) from the magnetic axis ($r = 0$), and integrating to the edge of the plasma ($r = 1$), we obtain the complex *plasma response parameter*

$$s(\gamma) = -\frac{1}{2}\left[1 + m^{-1}\,\frac{d\ln(Q\,\phi)}{d\ln r}\right]_{r=1}. \tag{4}$$

This parameter fully specifies the response of the plasma to the RWM.

B. Plasma stability parameter

The marginally stable ideal eigenmode equation

$$r\,\frac{d}{dr}\left(Q^2\,r\,\frac{d\phi}{dr}\right) - \left(m^2\,Q^2 + r\,\frac{dQ^2}{dr}\right)\phi = 0, \tag{5}$$

is obtained from Eq. (3) by neglecting plasma inertia, and governs the stability of the ideal external-kink mode.[19] Calculating the plasma response parameter (4) from the above equation, we obtain a real number, s_b, which is equivalent to the well-known Boozer stability parameter for the ideal external-kink mode.[20] It can be demonstrated that the m, n ideal external-kink mode is unstable when the wall is absent if $s_b > 0$, and is unstable even if the wall is perfectly conducting when $s_b > s_c \equiv c/(1-c)$.[19,20] Hence, we can define a real *plasma stability parameter*

$$\bar{s} = \frac{s_b}{s_c}. \tag{6}$$

The so-called *no-wall stability limit* corresponds to $\bar{s} = 0$, whereas the *perfect-wall stability limit* corresponds to $\bar{s} = 1$.

C. Vacuum solution

In the vacuum region external to the plasma (i.e., $r > 1$), the safety-factor profile takes the form $q = q_a\,r^2$, which implies that

$$\frac{d}{dr}\left[\frac{1}{r}\,\frac{d}{dr}\,(r^2\,Q)\right] = 0. \tag{7}$$

Equation (5), which also holds in the vacuum region, can be combined with Eq. (7) to give

$$r\,\frac{d}{dr}\left(r\,\frac{d\psi}{dr}\right) - m^2\,\psi = 0, \tag{8}$$

where $\psi = Q\,\phi$ is the perturbed poloidal magnetic flux associated with the RWM.

Suppose that the external region is bisected by a uniform, rigid wall (concentric with the edge of the plasma), of electrical conductivity σ_w, whose inner and outer surfaces correspond to $r = r_w$ and $r = r_w + \delta_w$, respectively (where $r_w > 1$). In the vacuum region between the plasma and the wall (i.e., $1 < r < r_w$), Eq. (8) leads to

$$\psi(r) = A\,r^m + B\,r^{-m}, \tag{9}$$

where A and B are arbitrary constants. Continuity of $d\ln\psi/d\ln r$ (i.e., continuity of both ψ and $d\psi/dr$, which implies the absence of current sheets) at the edge of the plasma yields

$$-m^{-1}\,\frac{d\ln\psi}{d\ln r}\bigg|_{r=1} = 1 + 2\,s, \tag{10}$$

where s is the complex plasma stability parameter defined in Eq. (4). It follows that

$$\psi(r) = B\left(-\frac{s}{1+s}\,r^m + r^{-m}\right), \tag{11}$$

and, hence, that

$$-m^{-1}\,\frac{d\ln\psi}{d\ln r}\bigg|_{r=r_w} = \frac{2\,s}{c - (1-c)\,s} + 1, \tag{12}$$

where

$$c = r_w^{-2\,m}. \tag{13}$$

In the vacuum region outside the wall (i.e., $r > r_w + \delta_w$), the solution to Eq. (8) that is well-behaved as $r \to \infty$ is

$$\psi(r) = C\,r^{-m}, \tag{14}$$

where C is an arbitrary constant. Hence,

$$-m^{-1}\,\frac{d\ln\psi}{d\ln r}\bigg|_{r=r_w+\delta_w} = 1. \tag{15}$$

D. Wall solution

Inside the wall, Eq. (8) takes the modified form

$$r\,\frac{d}{dr}\left(r\,\frac{d\psi}{dr}\right) - (m^2 + p^2\,r^2)\psi = 0, \tag{16}$$

where

$$p = (\gamma\,\mu_0\,\sigma_w)^{1/2}. \tag{17}$$

The general solution to Eq. (16) is

$$\psi(r) = D\, I_m(p\, r) + E\, K_m(p\, r), \tag{18}$$

where $I_m(z)$ and $K_m(z)$ are modified Bessel functions, and D and E are arbitrary constants. Making use of the well-known identities

$$I'_m(z) = I_{m-1}(z) - \frac{m}{z}\, I_m(z), \tag{19}$$

$$K'_m(z) = -K_{m-1}(z) - \frac{m}{z}\, K_m(z), \tag{20}$$

where $'$ denotes a derivative with respect to argument, we deduce that

$$-m^{-1}\, \frac{d\ln\psi}{d\ln r} = \frac{p\, r}{m}\, \frac{E\, K_{m-1}(p\, r) - D\, I_{m-1}(p\, r)}{E\, K_m(p\, r) + D\, I_m(p\, r)} + 1 \tag{21}$$

within the wall.

E. RWM dispersion relation

Asymptotically matching (i.e., demanding continuity of $d\ln\psi/d\ln r$) the wall solution, (18), to the vacuum solution at the inner and outer boundaries of the wall, making use of Eqs. (12), (15), and (21), we obtain the RWM dispersion relation[21]

$$\frac{s(\gamma)}{c - (1-c)\, s(\gamma)} = \frac{z_1}{2\, m}\, \frac{I_{m-1}(z_2)\, K_{m-1}(z_1) - K_{m-1}(z_2)\, I_{m-1}(z_1)}{I_{m-1}(z_2)\, K_m(z_1) + K_{m-1}(z_2)\, I_m(z_1)}, \tag{22}$$

where

$$z_1 = \left(2\, m\, \frac{\gamma}{\gamma_w}\, \frac{1}{\epsilon_w}\right)^{1/2}, \tag{23}$$

$$z_2 = z_1\, (1 + \epsilon_w), \tag{24}$$

and

$$\gamma_w = \frac{2\, m}{\sigma_w\, r_w\, \delta_w}, \tag{25}$$

$$\epsilon_w = \frac{\delta_w}{r_w}. \tag{26}$$

Here, γ_w is a typical (normalized) RWM growth-rate in the thin-wall limit, and ϵ_w is a measure of the relative wall thickness.

In the so-called *thin-wall limit*, $|z_1|\, \epsilon_w \ll 1$, in which the wall thickness is much less than the electromagnetic skin-depth in the wall material, the above dispersion relation reduces to[18]

$$\frac{s}{c - (1-c)\, s} = \frac{\gamma}{\gamma_w}. \tag{27}$$

On the other hand, in the so-called *thick-wall limit*, $|z_1|\, \epsilon_w \gg 1$, in which the wall thickness greatly exceeds the skin-depth, we get[22]

$$\frac{s}{c - (1-c)\, s} = \left(\frac{1}{2\, m}\, \frac{\gamma}{\gamma_w}\, \frac{r_w}{\delta_w}\right)^{1/2}. \tag{28}$$

III. NUMERICAL RESULTS

A. Calculation parameters

The calculations described in this paper were all performed using parameters appropriate to a predominately $m = 3$, $n = 1$ RWM in a typical DIII-D plasma. The DIII-D tokamak has major radius $R_0 = 1.69\,\mathrm{m}$, minor radius $a = 0.61\,\mathrm{m}$, typical on-axis toroidal field-strength $B_0 = 2.1\,\mathrm{T}$, and typical on-axis electron number density $n_0 = 6 \times 10^{19}\,\mathrm{m}^{-3}$.[23] It follows that $\tau_H = 3 \times 10^{-7}\,\mathrm{s}$. The typical electron number density, electron temperature, and ion temperature at the edge of a DIII-D discharge are $n_e = 2 \times 10^{19}\,\mathrm{m}^{-3}$, $T_e = 100\,\mathrm{eV}$, and $T_i = 100\,\mathrm{eV}$, respectively.[24] This implies that $\mu_\parallel = 1 \times 10^{-4}$ (in normalized units).[18]

The DIII-D wall parameters, c and γ_w, were determined by fitting to data obtained from the Valen code,[25] which calculates the RWM growth-rate as a function of the Boozer stability parameter, s_b, for a dissipationless plasma, and accurately models the DIII-D wall in three-dimensions via a finite-element representation that employs a standard thin-shell integral formulation. The fitting procedure (which was performed for a predominately 3, 1 mode) yields $c = 0.14$ and $\gamma_w = 8 \times 10^{-5}$ (in normalized units).[18]

According to Eq. (13), the effective radius of the DIII-D wall (for a 3, 1 RWM) is $r_w = c^{-1/6} = 1.39$ (in normalized units). Given that the wall is fabricated from Inconel 625,[26] which has an electrical resistivity of $\eta_w = \sigma_w^{-1} = 1.26 \times 10^{-6}\,\Omega\,\mathrm{m}$, it follows from Eq. (25) that $\gamma_w = 3.5 \times 10^{-6}\, \delta_w^{-1}$ (in normalized units), which implies that the effective thickness of the wall is $\delta_w = 4.4 \times 10^{-2}$ (in normalized units). Hence, from Eq. (26), the appropriate wall thickness parameter for a 3, 1 RWM in a DIII-D plasma is $\epsilon_w = 3.2 \times 10^{-2}$.

The stability boundaries for a 3, 1 RWM in a DIII-D discharge were determined numerically by adjusting the central safety-factor, q_0, and the (normalized) plasma toroidal angular velocity Ω_ϕ, until the RWM dispersion relation (22) yielded a purely imaginary growth-rate.

B. Results

Figure 1 shows the calculated stability boundary of the 3, 1 RWM in a typical DIII-D plasma, plotted in ideal plasma stability, $\bar{s}$, versus normalized plasma toroidal angular velocity, Ω_ϕ, space, for various different values of the wall thickness parameter ϵ_w. Note that varying ϵ_w, while keeping γ_w fixed, is equivalent to replacing the DIII-D wall with one of a different thickness that possesses the same overall electrical resistance.

The solid curve corresponds to the thin-wall limit. It can be seen that, in this limit, the RWM is stabilized once the plasma toroidal rotation velocity exceeds a critical value that is about 0.6% of the Alfvén velocity. Moreover, this stabilization extends almost all of the way to the perfect-wall stability boundary, $\bar{s} = 1$, which implies that the effective

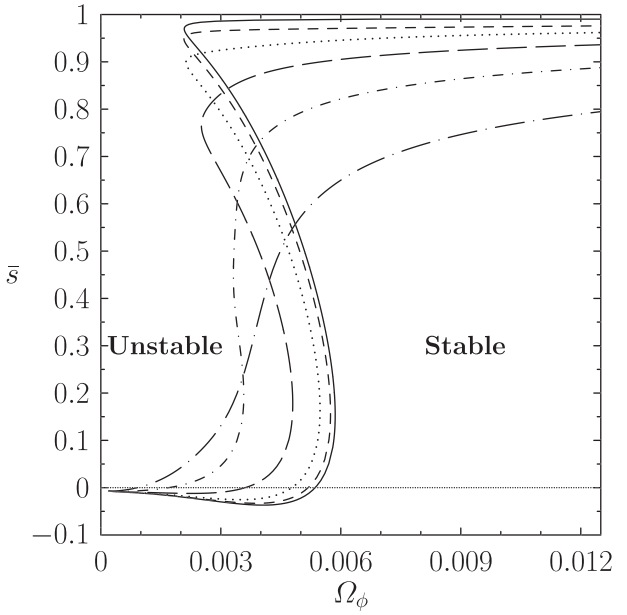

FIG. 1. RWM stability boundary plotted in normalized plasma toroidal angular velocity versus ideal plasma stability space. The calculation parameters are $m=3$, $n=1$, $\alpha=0.5$, $q_a=2.95$, $\epsilon_0=0.32$, $\mu_\parallel=1\times10^{-4}$, $c=0.14$, and $\gamma_w=8\times10^{-5}$. The solid, dashed, dotted, long-dashed, dashed-dotted, and long-dashed-dotted curves correspond to $\epsilon_w=10^{-3}$, 10^{-2}, $10^{-3/2}$, 10^{-1}, $10^{-1/2}$, and 10^{+0}, respectively. The no-wall and perfect-wall stability boundaries lie at $\bar{s}=0$ and $\bar{s}=1$, respectively.

β-limit of the rotationally stabilized plasma is the perfect-wall β-limit.

The dotted curve corresponds to the actual DIII-D wall, which possesses a finite thickness. It can be seen that the finite thickness of the DIII-D wall makes very little difference to the RWM stability boundary, which is almost the same as that calculated in the thin-wall limit. This suggests that the conventional thin-wall approximation is perfectly adequate for calculating RWM stability boundaries in present-day tokamaks.

The long-dashed, dashed-dotted, and long-dashed-dotted curves correspond to walls that are much thicker than the DIII-D wall (but have the same electrical resistance). It can be seen that, close to the no-wall stability boundary, $\bar{s}=0$, the critical plasma toroidal rotation velocity needed to stabilize the RWM is reduced in the presence of a thick wall (relative to that needed to stabilize the mode in the presence of thin wall of the same electrical resistance). On the other hand, close to the perfect-wall stability boundary, $\bar{s}=1$, the critical rotation velocity is increased in the presence of a thick wall. In fact, it is clear from the figure that a thick wall significantly impedes the ability of plasma rotation to stabilize the RWM all the way to the perfect-wall stability boundary. This suggests that the effective β-limit for a plasma in which the RWM is rotationally stabilized is significantly lower in the presence of a thick wall, relative to that in the presence of a thin wall of the same electrical resistance.

Figures 2 and 3 display the results of calculations that are similar to those shown in Fig. 1, except that the plasma edge safety-factor is slightly smaller. Lowering the edge-q tends to increase the critical plasma toroidal angular velocity needed to stabilize the RWM (which is of order $k_\parallel v_A$ at the

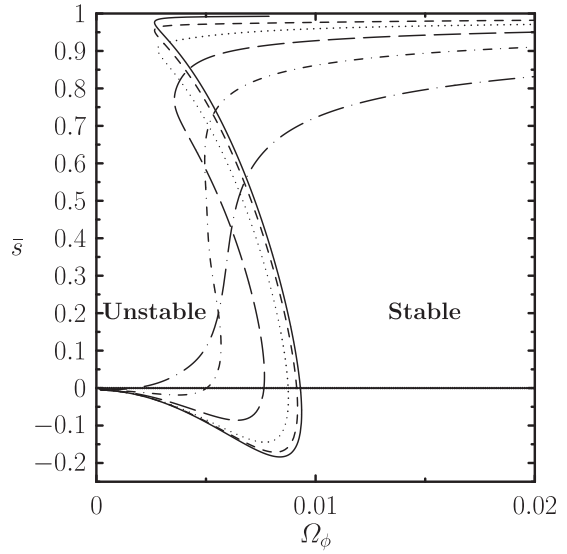

FIG. 2. RWM stability boundary plotted in normalized plasma toroidal angular velocity versus ideal plasma stability space. The calculation parameters are $m=3$, $n=1$, $\alpha=0.5$, $q_a=2.94$, $\epsilon_0=0.32$, $\mu_\parallel=1\times10^{-4}$, $c=0.14$, and $\gamma_w=8\times10^{-5}$. The solid, dashed, dotted, long-dashed, dashed-dotted, and long-dashed-dotted curves correspond to $\epsilon_w=10^{-3}$, 10^{-2}, $10^{-3/2}$, 10^{-1}, $10^{-1/2}$, and 10^{+0}, respectively. The no-wall and perfect-wall stability boundaries lie at $\bar{s}=0$ and $\bar{s}=1$, respectively.

edge of the plasma[22]). Furthermore, increasing the plasma rotation has the effect of accentuating the inertial destabilization of the RWM, which occurs at intermediate rotation levels, and leads to the RWM stability boundary dipping below the no-wall stability boundary ($\bar{s}=0$).[22] It can be seen that, in the presence of a thick wall, the inertial destabilization of the RWM at intermediate rotation levels is almost entirely

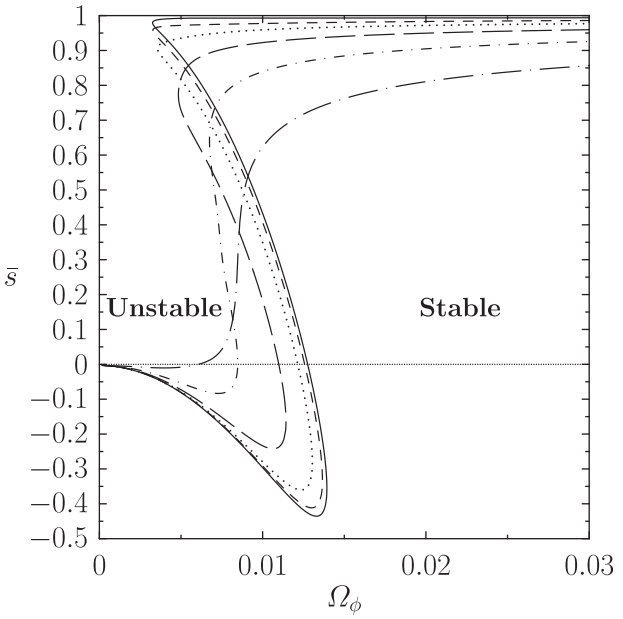

FIG. 3. RWM stability boundary plotted in normalized plasma toroidal angular velocity versus ideal plasma stability space. The calculation parameters are $m=3$, $n=1$, $\alpha=0.5$, $q_a=2.93$, $\epsilon_0=0.32$, $\mu_\parallel=1\times10^{-4}$, $c=0.14$, and $\gamma_w=8\times10^{-5}$. The solid, dashed, dotted, long-dashed, dashed-dotted, and long-dashed-dotted curves correspond to $\epsilon_w=10^{-3}$, 10^{-2}, $10^{-3/2}$, 10^{-1}, $10^{-1/2}$, and 10^{+0}, respectively. The no-wall and perfect-wall stability boundaries lie at $\bar{s}=0$ and $\bar{s}=1$, respectively.

eliminated. In other respects, the effect of a thick wall is the same as that shown in Fig. 1.

IV. SUMMARY

We have determined the influence of finite wall thickness on the stability of the RWM in a tokamak using a previously published[16–18] cylindrical plasma model in which the dissipation required to stabilize the mode is provided by neoclassical parallel ion viscosity. We find that for present-day tokamaks, such as DIII-D, which possess relatively thin walls, finite wall thickness effects have relatively little influence on the RWM stability boundary, which is almost the same as that calculated in the thin-wall limit. We also find that for next-step devices, such as ITER, which are likely to possess much thicker walls than present-day tokamaks, finite wall thickness effects can significantly impede the ability of plasma rotation to stabilize the RWM all the way to the perfect-wall stability boundary. Finally, we find that thick walls decrease the critical plasma rotation needed to stabilize the RWM close to the no-wall stability boundary, and also suppress any inertial destabilization of the mode at intermediate rotation levels.

One obvious question is the extent to which the conclusions of this paper are dependent on the damping model. The neoclassical model used in this paper was selected because it is extremely simple (which is an important consideration, since the stability diagrams shown in the figures required hundreds of solutions of the RWM dispersion relation), and yet leads to RWM stability boundaries that are broadly consistent with those observed in conventional tokamaks such as DIII-D and HBT-EP.[17] In recent years, various researchers have developed a drift-kinetic damping model for the RWM.[27–29] This model, which is significantly more complicated than the neoclassical model, has been highly successful at explaining the RWM stability boundaries observed in low aspect-ratio tokamaks such as NSTX.[30] It is interesting to note that the drift-kinetic damping model leads to a cubic dispersion relation (with two roots rotating with the plasma, one leading and one lagging, and one slowly rotating root that can be identified as the RWM),[31,32] in accordance with results obtained using simple damping models[22] (including the model adopted in this paper—we have simply not talked about the rotating roots, because they are always stable). This encourages us to hope that the conclusions of this paper are generic, and are not specific to the adopted damping model.

ACKNOWLEDGMENTS

This research was funded by the U.S. Department of Energy under Contract DE-FG02-04ER-54742.

[1]F. Troyon, R. Gruber, H. Saurenmann, S. Semenzato, and S. Succi, Plasma Phys. Controlled Fusion **26**, 209 (1984).
[2]C. Kessel, J. Manickam, G. Rewoldt, and W. M. Tang, Phys. Rev. Lett. **72**, 1212 (1994).
[3]E. A. Lazarus, G. A. Navratil, C. M. Greenfield *et al.*, Phys. Rev. Lett. **77**, 2714 (1996).
[4]J. P. Goedbloed, D. Pfirsch, and H. Tasso, Nucl. Fusion **12**, 649 (1972).
[5]M. Okabayashi, N. Pomphrey, J. Manikam *et al.*, Nucl. Fusion **36**, 1167 (1996).
[6]A. M. Garofalo, E. Eisner, T. H. Ivers *et al.*, Nucl. Fusion **38**, 1029 (1998).
[7]A. M. Garofalo, E. J. Strait, L. C. Johnson *et al.*, Phys. Rev. Lett. **89**, 235001 (2002).
[8]S. A. Sabbagh, J. M. Bialek, R. E. Bell *et al.*, Nucl. Fusion **44**, 560 (2004).
[9]M. Shilov, C. Cates, R. James *et al.*, Phys. Plasmas **11**, 2573 (2004).
[10]A. Bondeson and D. J. Ward, Phys. Rev. Lett. **72**, 2709 (1994).
[11]R. Betti and J. P. Freidberg, Phys. Rev. Lett. **74**, 2949 (1995).
[12]R. Aymar, P. Barabashchi, and Y. Shimomura, Plasma Phys. Controlled Fusion **44**, 519 (2002).
[13]L.-J. Zheng and M. T. Kotschenreuther, Phys. Plasmas **12**, 072504 (2005).
[14]L. X. Chen and Z. W. Ma, Phys. Scr. **84**, 025504 (2011).
[15]V. D. Pustovitov, Phys. Plasmas **19**, 062503 (2012).
[16]K. C. Shaing, Phys. Plasmas **11**, 5525 (2004).
[17]R. Fitzpatrick and J. Bialek, Phys. Plasmas **13**, 072512 (2006).
[18]R. Fitzpatrick, Phys. Plasmas **14**, 022505 (2007).
[19]W. A. Newcomb, Ann. Phys. (N.Y.) **10**, 232 (1960).
[20]A. H. Boozer, Phys. Plasmas **5**, 3350 (1998).
[21]G. F. Nalesso and S. Costa, Nucl. Fusion **20**, 443 (1980).
[22]R. Fitzpatrick and A. Y. Aydemir, Nucl. Fusion **36**, 11 (1996).
[23]H. Remierdes, T. C. Hender, S. A. Sabbagh *et al.*, Phys. Plasmas **13**, 056107 (2006).
[24]W. M. Stacey and R. J. Groebner, Phys. Plasmas **13**, 012513 (2006).
[25]J. Bialek, A. H. Boozer, M. E. Mauel, and G. A. Navratil, Phys. Plasmas **8**, 2170 (2001).
[26]P. W. Trester, J. L. Kaae, and R. Gallix, J. Nucl. Mater. **133–134**, 347 (1985).
[27]A. Bondeson and M. S. Chu, Phys. Plasmas **3**, 3013 (1996).
[28]B. Hu and R. Betti, Phys. Rev. Lett. **93**, 105002 (2004).
[29]Y. Liu, M. S. Chu, I. T. Chapman, and T. C. Hender, Phys. Plasmas **15**, 112503 (2008).
[30]J. W. Berkery, S. A. Sabbagh, R. Betti, R. E. Bell, S. P. Gerhardt, B. P. LeBlanc, and H. Yuh, Phys. Rev. Lett. **106**, 075004 (2011).
[31]Y. Liu, I. T. Chapman, M. S. Chu *et al.*, Phys. Plasmas **16**, 056113 (2009).
[32]J. W. Berkery, R. Betti, and S. A. Sabbagh, Phys. Plasmas **18**, 072501 (2011).